



### **Science Arts & Métiers (SAM)**

is an open access repository that collects the work of Arts et Métiers Institute of Technology researchers and makes it freely available over the web where possible.

This is an author-deposited version published in: <https://sam.ensam.eu>  
Handle ID: [.http://hdl.handle.net/10985/10213](http://hdl.handle.net/10985/10213)

#### **To cite this version :**

Seifeddine BENELGHALI, Jean-Frederic CHARPENTIER, Mohamed BENBOUZID - Ressource to wire modelling for tidal turbines - 2013

Any correspondence concerning this service should be sent to the repository

Administrator : [scienceouverte@ensam.eu](mailto:scienceouverte@ensam.eu)



## 9.1 Resource to wire modelling for tidal turbines

*S. Benelghali, JF Charpentier, and M. Benbouzid*

### Nomenclature

$\rho$	Fluid density
$A$	Cross-sectional area of the marine turbine
$V_{\text{tide}}$	Fluid speed
$C_p$	Power coefficient
$\beta$	Pitch angle
$C$	Tide coefficient
$V_{\text{st}} (V_{\text{nt}})$	Spring (neap) tide current speed
$\lambda$	Tip speed ratio
$s, (r)$	Stator (rotor) index (superscripts)
$d, q$	Synchronous reference frame index
$V (I)$	Voltage (current)
$P (Q)$	Active (reactive) power
$\phi$	Flux
$\phi_m$	Permanent magnet flux
$T_{em} (T_m)$	Electromagnetic torque (mechanical torque)
$R$	Resistance
$L (M)$	Inductance (mutual inductance)
$\sigma$	Total leakage coefficient, $\sigma = 1 - M^2/L_s L_r$
$\theta_r$	Rotor position
$\omega (\omega_s)$	Rotor electrical speed (electrical synchronous speed)
$\omega_r$	Rotor current frequency ( $\omega_r = \omega_s - \omega$ )
$\Omega$	Mechanical speed ( $\Omega = \omega/p$ )
$f$	Viscosity coefficient
$J$	Rotor inertia

$p$	Pole pair number
$L_{ss}$	Stator inductance
$M_s$	Stator mutual magnetizing inductance
$M_{jr}$	Rotor mutual magnetizing inductance in phase $j, j=a, b$ or $c$
$\lambda_j$	PMSG rotor flux in phase $j, j=a, b$ or $c$

### 9.1.1 Modelling requirements

Tidal turbine dynamic performance analysis requires the use of computational models representing the nonlinear differential-algebraic equations of the various system components such as tidal resource, turbine, generator, converter, control system and grid connection, as shown in Figure 9.1. However, the main difficulty is to include a variety of sub-models with different timescales for hydrodynamic loads (turbine, mechanical systems, generators, power electronics and other components). The user is therefore concerned with selecting the appropriate models for the problem at hand and determining the data to represent the specific turbine equipment.

Appropriate model choice depends mainly on the timescale of the simulation. Figure 9.2 shows the principal tidal turbine dynamic performance areas displayed on a logarithmic timescale ranging from microseconds to days. The lower end of the band for a particular item indicates the smallest time constants that need to be included for a precise modelling of each element.

The upper end indicates the approximate length of time that must be analysed. It is possible to build a turbine simulation model that includes all dynamic effects from very fast dynamics to very slow hydrodynamic loads; however, this solution can be highly time consuming to develop and execute. For efficiency and ease of analysis, normal engineering practice dictates that only models incorporating dynamic effects relevant to the particular performance of the concerned area to be used. Some basic models of each subsystem will be presented in the next section: resource, turbine, generator and converter.

### 9.1.2 Resource modelling

First of all, a basic model of the tidal resource is presented. The proposed method is illustrated by the calculation of the extractable power from the Raz de Sein (Brittany, France) as it is one of the more characterized sites in terms of tidal

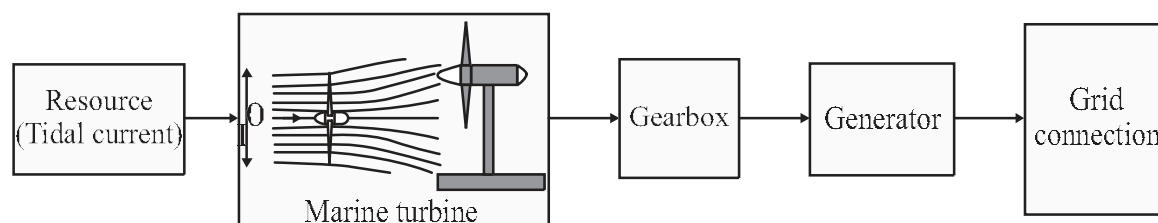


Figure 9.1 *Tidal turbine global scheme*

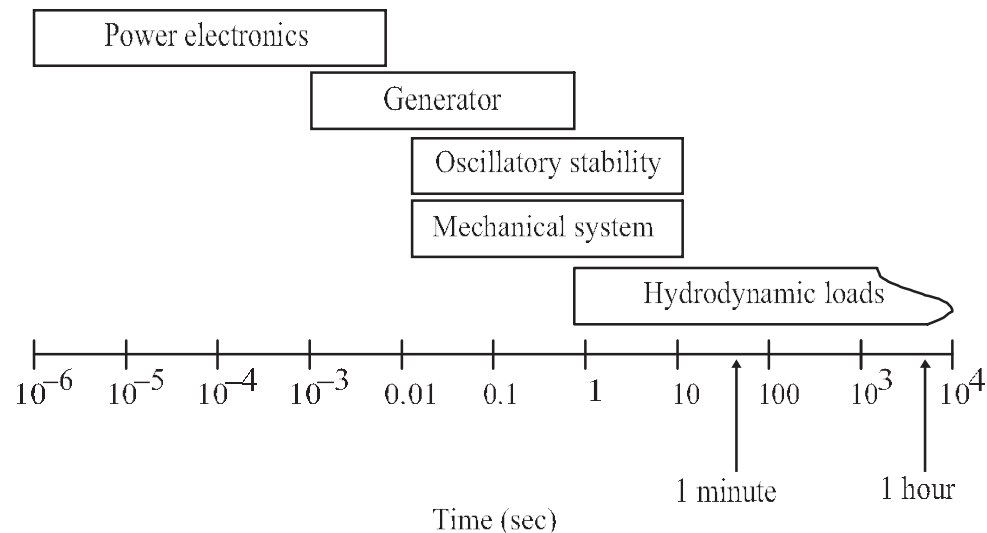


Figure 9.2 Timescale in a tidal turbine

current. The following modelling approach can be extended to any other sites. This site was chosen above several others listed in the European Commission report EUR16683 due to the presence of high velocity current coupled with appropriate depths suitable for tidal turbine [1]. Moreover, the marine current velocity distribution for most of the time is greater than the minimum velocity required for economic deployment of marine turbines, estimated to be 1 m/s [1, 2]. It should be noted that tidal current data are provided by the SHOM (French Navy Hydrographic and Oceanographic Service) and it is available for various locations in chart form [3].

Oceanographic services (such as the French SHOM for the illustration site) produce charts giving the current velocities for spring and neap tides at a specific site. These values are given at hourly intervals starting at 6 tidal hours before high waters and ending 6 hours after (tide hours). Therefore, knowing tide coefficients, it is easy to derive a simple and practical model to calculate the tidal current velocity vector for each tidal hour for a given coefficient  $V_{tide}(Hm, C)$ , where  $Hm$  is the tidal hour (i.e. the time defined by the semidiurnal tide period divided by 12) [10].

$$\vec{V}_{tide}(Hm, C) = \vec{V}_{nt}(Hm) + \frac{(C - 45)(\vec{V}_{st} - \vec{V}_{nt})}{95 - 45} \quad (9.1)$$

$C$  is the coefficient that characterises each tidal cycle (95 and 45 are, respectively, the spring and neap tide medium coefficient). This coefficient is determined by the astronomic calculation of earth and moon positions.  $V_{st}$  and  $V_{nt}$  are, respectively, the spring and neap tide current velocities for hourly intervals starting at 6 hours before high waters and ending 6 hours after.

For example, consider the case of a semidiurnal cycle that is characterised by a tide coefficient of  $C=80$  in a given geographical point. At this point, 3 hours after high tide, the data charts give  $V_{st}=1.8$  knots and  $V_{nt}=0.9$  knots, thus the speed calculated using (9.1) is  $V_{tide}=1.53$  knots. This first-order model is then used to calculate the tidal velocity vector for each hour. The implemented model will allow

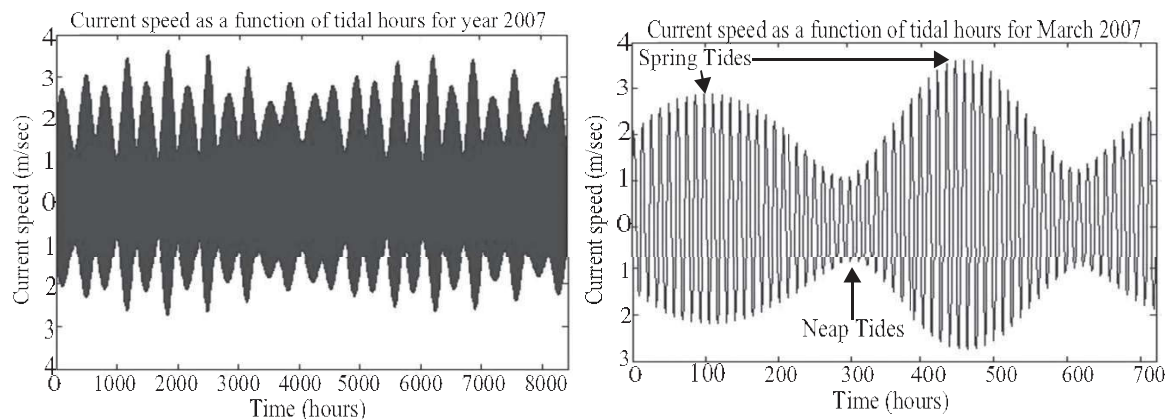


Figure 9.3 Tidal velocity in the Raz de Sein for the year 2007 and March 2007

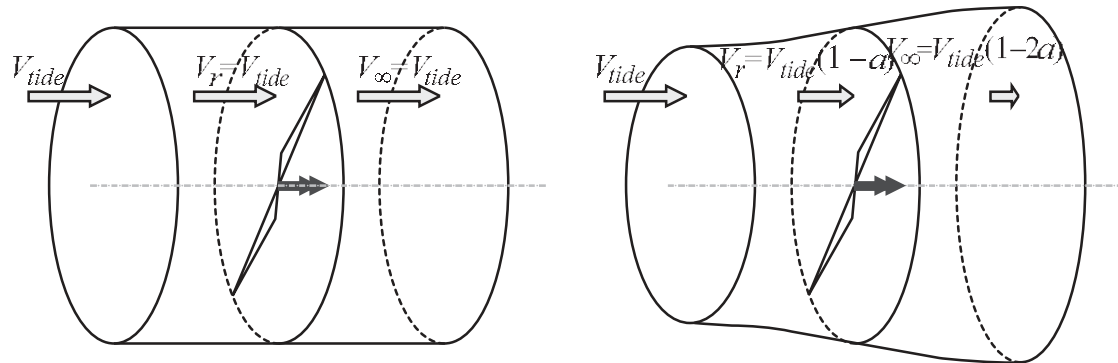
the user to compute tidal velocities in a predefined time range. Figure 9.3 shows the model output for a month (March 2007) and for a year (2007).

The first-order model which has been adopted for the resource has several advantages including its modularity and its simplicity. Indeed, the marine turbine site can be changed, the useful current velocity can be varied, and the time range taken into account can also be altered from one month to one year. For a simulation of short periods (less than a few minutes), the tidal velocity can be considered as constant. However, some faster disturbances such as swell effects and turbulence can also be taken into account for a greater level of accuracy.

### 9.1.3 Hydrodynamic modelling of an horizontal axis turbine

Several technologies have been proposed to convert tidal power into electrical power. Most of them are based upon the use of horizontal axis turbines [4], which have been successfully utilized to harness wind energy [3]. Therefore, many techniques can be transferred from the design and operation of wind turbines [5]. There are, however, a number of fundamental differences in the design and operation of marine turbines. Particular differences entail changes in force loadings, immersion depth, different stall characteristics, and the possible occurrence of a cavitation phenomenon in the blades.

A first theoretical analysis of the hydrodynamic behaviour of a turbine can be done using the Rankine–Froude actuator disc model. This model consists of replacing the rotor with a theoretical actuator disc, which is a circular surface of zero thickness that can support a pressure difference, and thus decelerate the tidal current through the disc. The principal use of the actuator disc model is to obtain a first estimate of the wake-induced flow, and hence the total induced power loss. Note that the actual induced power loss will be larger than the actuator disk result because of the non-uniform and unsteady induced velocity. The assumptions on which the Rankine–Froude actuator disc theory is based are well-detailed in [5]. Among these assumptions, one requires that the disc slows the tidal current equally at each radius, which is equivalent to assuming uniform thrust loading at the disc.



Tidal turbine with (right) and without (left) loading.

Figure 9.4 The actuator disk model

Uniform thrust loading is, in turn, equivalent to considering an infinite number of rotor blades.

Figure 9.4 illustrates the one-dimensional flow through the actuator disc plane for a non-loaded and loaded machine. For instance, for a turbine with zero loading, the current velocity in the rotor plane ( $V_r$ ) is equal to the undisturbed tidal current velocity ( $V_{tide}$ ); while for a loaded turbine, the rotor current velocity is reduced. If the decreased velocity induced by the rotor is  $V$ , then the velocity at the disk is  $V_{tide} - V = V_r$  and far downstream, at section 1, the current has been slowed further to velocity  $V_\infty$ . The difference between the axial component of the current velocity and the axial flow velocity in the rotor plane is usually called *induced velocity*. Thus, the velocity at the disc is the average of the upstream and downstream velocities. Defining an axial induction factor,  $a$ , as the fractional decrease in current velocity between the free stream and the rotor plane represented by (9.2)

$$a = \frac{V}{V_{tide}} \quad (9.2)$$

The results in (9.3):

$$\begin{cases} V_r = V_{tide}(1-a) \\ V_\infty = V_{tide}(1-2a) \end{cases} \quad (9.3)$$

For  $a=0$ , the current is not decelerated and no power is extracted, whereas for  $a=0.5$ , the far wake velocity vanishes, and, without presence of flow behind the turbine, no power is generated. The power extracted from the tidal current by the rotor is given by (9.4)

$$P = \frac{1}{2} \rho A V_r (V - V_\infty) (V + V_\infty) \quad (9.4)$$

Substituting  $V_r$  and  $V_\infty$  from (9.3), we find that

$$P = \frac{1}{2} \rho A V_{tide}^3 4a(1-a)^2 \quad (9.5)$$



A power coefficient  $C_p$  is then defined as

$$C_p = \frac{P}{\frac{1}{2}\rho A V_{tide}^3} = 4a(1-a)^2 \quad (9.6)$$

where the denominator represents the global kinetic energy of the free-stream current contained in a stream tube with an area equal to the disk area. The extracted power is expressed by (9.7)

$$P = \frac{1}{2}\rho C_p A V_{tide}^3 \quad (9.7)$$

The theoretical maximum value of the power coefficient  $C_p$  occurs when  $a=1/3$ . Hence,  $C_{p,max} = 16/27 \approx 0.59259$ ,  $V_r = 2/3 V_{tide}$  and  $V_\infty = 1/3 V$ . Thus, the theoretical maximum amount of energy extraction equals the 16/27th part of the kinetic energy in the current. This limit is often referred to as the *Betz limit*, or more accurately the *Lanchester–Betz limit*. In practice this limit cannot be reached and the maximal values of the  $C_p$  of real turbines are often in the 0.4–0.5 range.

$C_p$  varies according to the pitch angle of the blades ( $\beta$ ) and the tip-speed ratio ( $\lambda$ ), where  $\lambda$  is the ratio between the tip-speed of the rotor and the tidal velocity. A  $C_p(\lambda, \beta)$  curve, such as the one shown in Figure 9.5, is typically developed by manufacturers as a means of characterizing the performance of the turbine.

This very simple model gives an indication of the turbine behaviour but is not sufficient to calculate the real performance of a given turbine for a working point (given blade shape and geometry and given flow and rotation speeds).

One of the more easily used models that can be used for this purpose is the blade element momentum (BEM) theory, which is one of the oldest and most commonly used methods for calculating induced velocities on wind turbine blades. This theory is an extension of the actuator disk theory [5, 9] extended to each blade sections. This theory is fully described in [11].

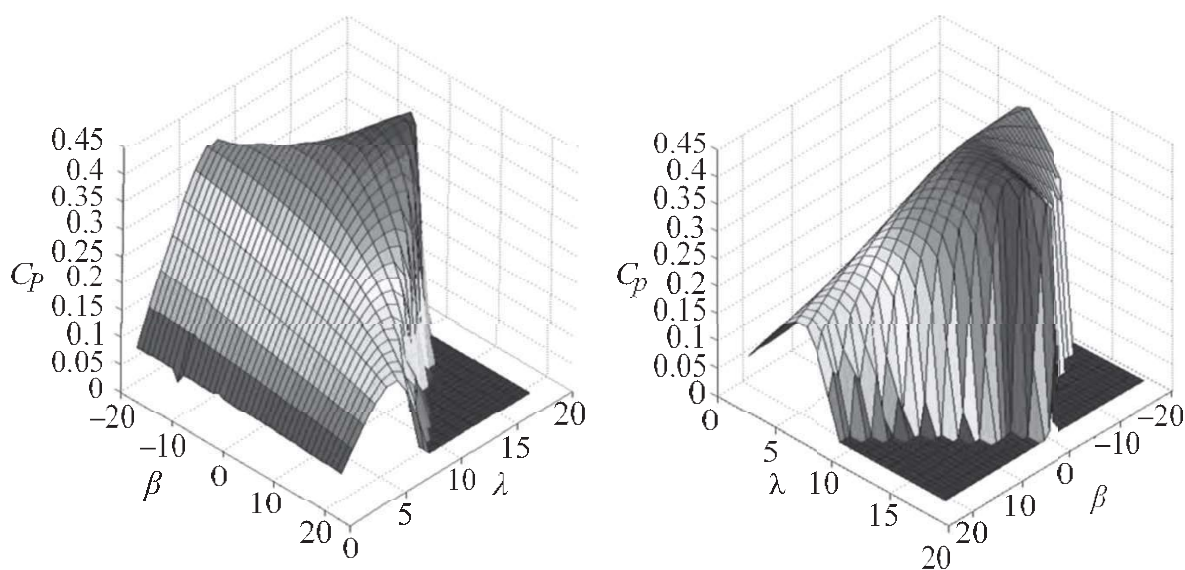


Figure 9.5  $C_p(\lambda, \beta)$  curves

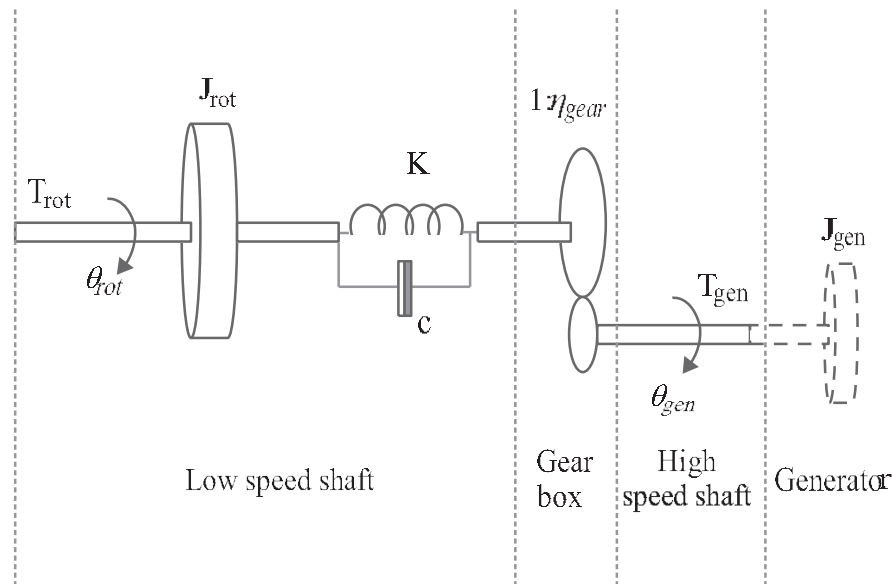


Figure 9.6 Drive train model

An example of simulation results using BEM theory, for a given three-blade turbine, is given by Figure 9.5, which presents the rotor power coefficient ( $C_p$ ) according to the pitch angle variation of the blades  $\beta$  and the speed ratio  $\lambda$ .

#### 9.1.4 Drive train modelling

For mechanical modelling, emphasis is put only on those parts of the dynamic structure of the marine current turbine that contributes to the interaction with the grid. Therefore, only the drive train is considered because this part of the marine turbine has the most significant influence on the power fluctuations. The structural components of the tidal turbines are not considered in this first order approach.

The mechanical drive train can be considered as a two-mass model, namely a large mass representing the rotor, and a smaller mass representing the generator. These rotating masses have inertia  $J_{rot}$  and  $J_{gen}$  respectively. The (low-speed) rotor shaft is connected to the (high-speed) generator shaft via a 1:N gearbox. The low-speed shaft is modelled by a stiffness  $k$  and a damping coefficient  $c$ , while the high-speed shaft is assumed stiff.

The drive train transfers the hydrodynamic rotor torque,  $T_{rot}$  to the low speed shaft torque  $T_{gen}$ . The mechanical model dynamical description consists of the following equations in (9.8)

$$\begin{cases} \dot{\theta}_{rot} = \omega_{rot} \\ \dot{\theta}_k = \omega_{rot} - \frac{\omega_{gen}}{\eta_{gear}} \\ \dot{\omega}_{rot} = \frac{(T_{rot} - T_{gen})}{J_{rot}} \end{cases} \quad (9.8)$$

where  $\theta_k$  is the angular difference between the two ends of the flexible shaft. For simplicity,  $\theta_k$  can be considered as a constant and the drive train model can be simplified as shown in Figure 9.7.



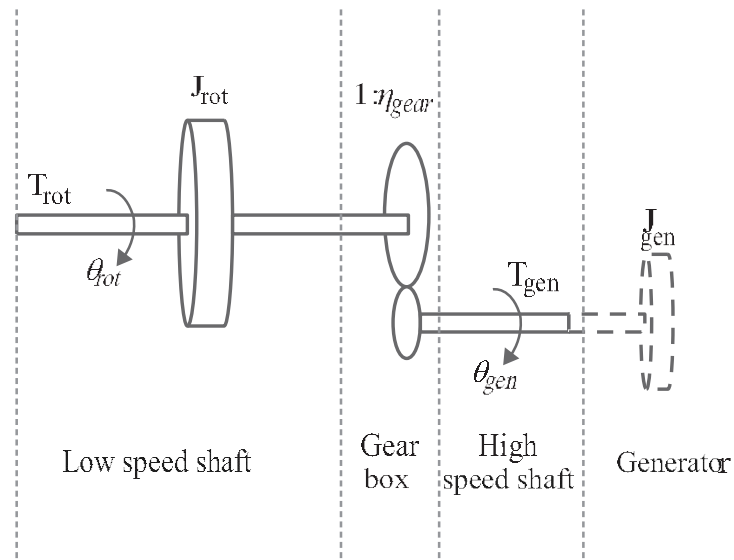


Figure 9.7 *Simplified drive train model*

### 9.1.5 Generator modelling

Much of the technology that has been suggested for tidal current energy extraction is comparable to that used in wind energy applications. It is then obvious that some wind generator topologies could be used for tidal turbines. This section will focus on modelling a PMSG associated with a back-to-back IGBT converter; other solutions based on Induction Generators or Double Fed Induction Generators (DFIG) can be modelled using similar methods.

For a PMSG, the stator voltage equations in stationary reference frame are given by (9.9)

$$[V_{abc}] = [R][i_{abc}] + [L]\frac{d[i_{abc}]}{dt} + \frac{d\lambda_{abc}}{dt} \quad (9.9)$$

where  $[L] = \begin{bmatrix} L_{ss} & M_s & M_s \\ M_s & L_{ss} & M_s \\ M_s & M_s & L_{ss} \end{bmatrix}$

The PMSG is modelled under the following simplifying assumptions:

- sinusoidal distribution of stator winding,
- electric and magnetic symmetry,
- negligible iron losses and unsaturated magnetic circuit.

Under these assumptions, the generator model in the so-called steady-state (or stator) coordinates is first obtained.

From (9.9), a simple model suitable for simulation and control can be obtained in  $d$ - $q$  rotor coordinates. Conversion between  $(a, b, c)$  and  $d$ - $q$  coordinates can be

AQ4

realized by means of the classical Park transform. Using this transform, the  $d$ - $q$  PMSG voltages and fluxes become

$$\begin{cases} V_d = Ri_d + L_d \frac{di_d}{dt} - L_q \dot{i}_q \omega_s \\ V_q = Ri_q + L_q \frac{di_q}{dt} + (L_d \dot{i}_d + \phi_m) \omega_s \end{cases} \quad (9.10)$$

The electromagnetic torque is obtained as in (9.11)

$$T_{em} = \frac{3}{2} p (\phi_d \dot{i}_q - \phi_q \dot{i}_d) = \frac{3}{2} p [\phi_m \dot{i}_q + (L_d - L_q) \dot{i}_d \dot{i}_q] \quad (9.11)$$

If the permanent magnets are mounted on the rotor surface, then  $L_d = L_q$  and the electromagnetic torque becomes (9.12)

$$T_{em} = \frac{3}{2} p \phi_m \dot{i}_q \quad (9.12)$$

This equation can be linked with the mechanical equation of the rotating parts (generator, rotor, drive train, turbine). As an example for a direct drive system the mechanical equation is

$$T_{gen} - T_{em} - T_l = J \frac{d\Omega_{gen}}{dt} \quad (9.13)$$

where  $T_{gen}$  is the mechanical torque which comes from the gearbox or directly from the turbine (in case of direct driven systems) and is an input for the generator. This torque can be deduced from the gearbox characteristics, the power curves of the turbines, the flow speed and the turbine rotational speed.  $T_l$  is a torque which represents the mechanical and iron losses.

Knowing the main electrical parameters of the generator ( $L_d$ ,  $L_q$ ,  $\phi_m$  and generator mechanical parameters), (9.10), (9.11) and (9.12) can be used to simulate the electromechanical behaviour of the generator. Of course, similar electromechanical models can be found and used for the other possible kind of generator (induction, double fed induction generator).

### 9.1.6 Global model of the system

It can be noted that for each model, input or output corresponds to output or input of others models. For example the input of the model of the turbine is the rotating speed related to the mechanical equation and current flow speed related to resource model. So the presented basic models can be associated in a modular environment dedicated for system simulation as for example the Matlab/Simulink environment. In this kind of environment, each of the previously described equation sets (resource, turbine, drive train, converter, or generator models) can be implemented in simulation blocks and connected to form a global simulation model. This allows for the calculation of the electrical and mechanical behaviour of the global system

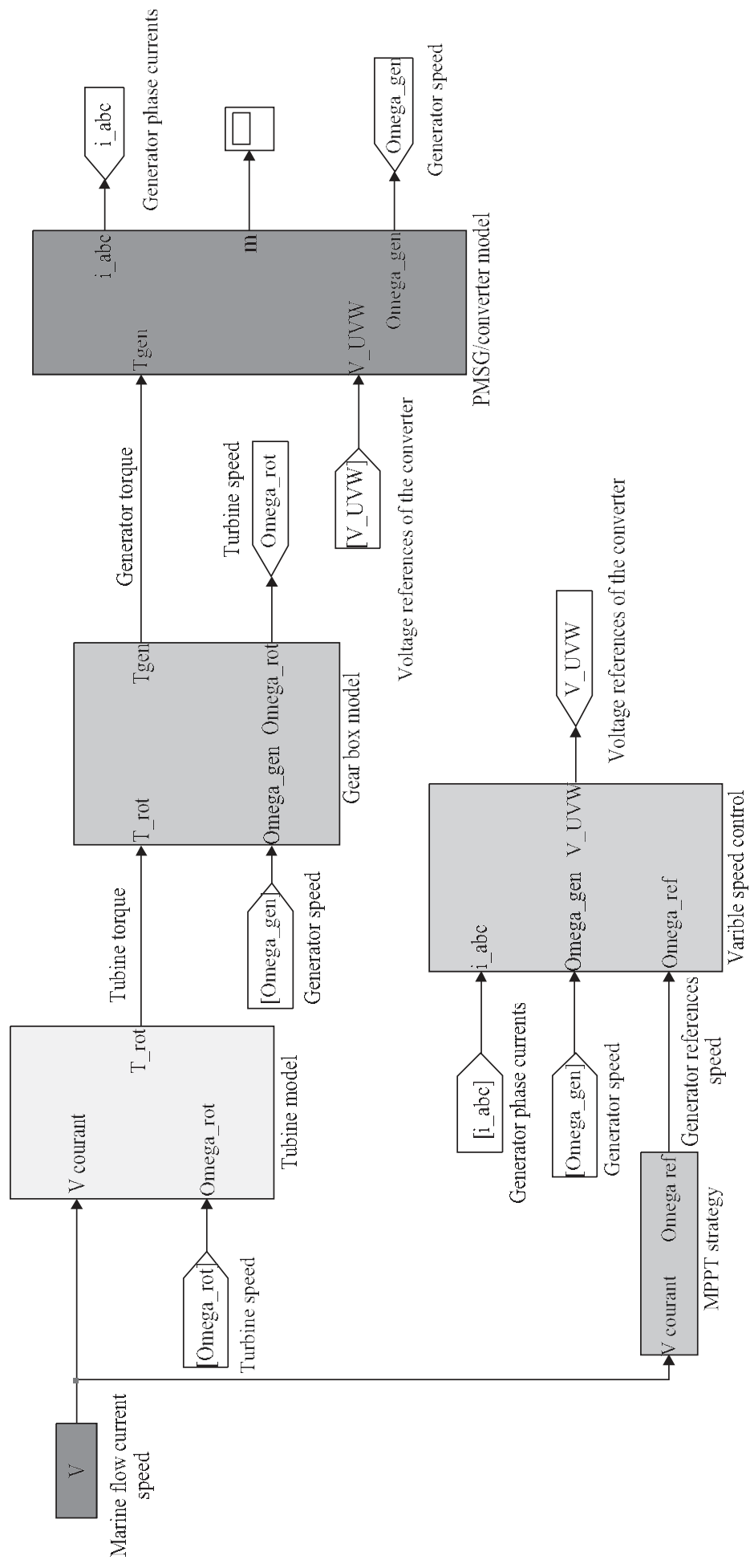


Figure 9.8 General view of a turbine simulation model in Matlab/Simulink environment